

MaskGAE: Masked Graph Modeling Meets Graph Autoencoders

Jintang Li^{*†‡}, Ruofan Wu^{*‡}, Jie Liao[†], Liang Chen[†], Sheng Tian[†], Liang Zhu[‡], Changhua Meng[‡],
Zibin Zheng[†], and Weiqiang Wang[‡]

[†]Sun Yat-sen University

[‡]Ant Group

{lijt55, liaoj27}@mail2.sysu.edu.cn

{chenliang6, zhizibin}@mail.sysu.edu.cn

{ruofan.wrf, tiansheng.ts, tiansheng.ts, changhua.mch, weiqiang.wq}@antgroup.com

Abstract

We present masked graph autoencoder (MaskGAE), a self-supervised learning framework for graph-structured data. Different from previous graph autoencoders (GAEs), MaskGAE adopts masked graph modeling (MGM) as a principled pretext task: masking a portion of edges and attempting to reconstruct the missing part with partially visible, unmasked graph structure. To understand whether MGM can help GAEs learn better representations, we provide both theoretical and empirical evidence to justify the benefits of this pretext task. Theoretically, we establish the connections between GAEs and contrastive learning, showing that MGM significantly improves the self-supervised learning scheme of GAEs. Empirically, we conduct extensive experiments on a number of benchmark datasets, demonstrating the superiority of MaskGAE over several state-of-the-arts on both link prediction and node classification tasks. Our code is publicly available at <https://github.com/EdisonLeeeee/MaskGAE>.

1 Introduction

Self-supervised learning, which learns broadly useful representations from unlabeled graphs in a task-agnostic way, has emerged as a popular and empirically successful learning paradigm for graph neural networks (GNNs) [47]. The key insight behind self-supervised learning is to obtain supervisory signals from the data itself with different handcrafted auxiliary tasks (so-called *pretext tasks*). The past few years have witnessed the success of graph self-supervised learning in a wide range of graph-related fields [42, 34, 52, 50], particularly chemical and biomedical science [29, 54], where label annotation can be very costly or even impossible to acquire.

For years, there are several research efforts in an attempt to exploit vast unlabeled data for self-supervised learning. Among contemporary approaches, contrast learning [42, 34, 52, 50] is one of the most widespread self-supervised learning paradigms on graph data. It learns representations that are invariant to different augmentation views of graphs, achieving remarkable success in various graph representation learning tasks [47]. Despite being effective and prevalent, graph contrastive methods highly rely on specialized and complex pretext tasks for self-supervised learning [16, 11], with data augmentation being crucial for contrasting different structural views of graphs [51, 19].

There is another prominent line of research attempts to learn representations through generative perspectives, with graph autoencoders as representative examples. Graph autoencoders (GAEs)

^{*}Equal contribution

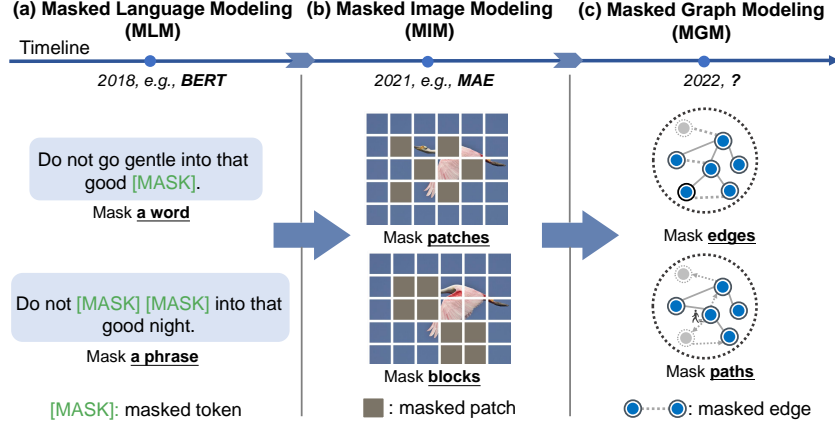


Figure 1: **From left to right:** illustrative examples of (a) masked language modeling (MLM), (b) masked image modeling (MIM), and (c) masked graph modeling (MGM) paradigms with different masking strategies. Similar to MLM and MIM, the goal of MGM is to learn representations by predicting randomly masked edges based on visible structure.

are a family of self-supervised learning models that take the graph input itself as self-supervision and learn to reconstruct the graph structure [18, 23]. Compared to contrastive methods, GAEs are generally very simple to implement and easy to combine with existing frameworks, since they naturally leverage graph reconstruction as pretext tasks without need of augmentations for view generations [47]. However, literature has shown that GAEs following such a simple graph-reconstruction principle might over-emphasize proximity information that is not always beneficial for self-supervised learning [42, 36, 11, 55], making it less applicable to other challenging tasks beyond link prediction. Therefore, there is a need for designing better pretext tasks for GAEs.

Masked autoencoding, whose goal is to reconstruct masked signals from unmasked input under the autoencoder framework, has recently advanced the state-of-the-art and provided valuable insights in both language and vision research. As shown in Figure 1(a) and 1(b), masked language modeling (MLM) and masked image modeling (MIM) have been widely applied to text and image data, with prominent examples including BERT [5] and MAE [12], respectively. Despite the fact that masked autoencoding has shown promise in benefiting visual and language representation learning, the applicability on graph data has yet to be substantially investigated in this discipline. Actually, masked autoencoding should also be a good fit for graph data, since each edge can easily be masked or unmasked as self-supervisions. In light of this, a natural question arises: *whether masked autoencoding, or masked graph modeling, would advance GAEs in self-supervised learning as well.*

Present work. In this work, we seek to continue the success of MLM and MIM by introducing masked graph modeling (MGM) as a principled pretext task for graph-structured data. As shown in Figure 1(c), the core idea behind MGM is to remove a portion of the input graph and learn to predict the removed content such as edges. Following this philosophy, we propose masked graph autoencoder (MaskGAE), a self-supervised learning framework that leverages the idea of masking and predicting through the node and edge-level reconstruction. Our framework is theoretically grounded by explicitly relating GAEs to contrastive learning and demonstrating the benefits of MGM in improving the self-supervised learning scheme of GAEs. Specifically, we reveal that the learning objective of GAEs is equivalent to contrastive learning, in which paired subgraphs naturally form two structural views for contrasting. Most importantly, masking on an edge can reduce redundancy for two contrastive subgraph views in GAEs and thus benefiting the contrastive scheme.

Main contributions. This paper offers the following main contributions: (i) MaskGAE, a simple and effective self-supervised learning framework for graphs; (ii) A comprehensive theoretical analysis of the proposed framework along with guidance on the design of pretext training task (i.e., MGM) for GAEs; (iii) A new form of structured masking strategy to facilitate MGM task, where edges in a contiguous region are masked together. (iv) An in-depth experimental evaluation of the proposed framework, demonstrating the effectiveness of MaskGAE on both link prediction and node classification tasks. We believe that our work is a step forward in the development of simple and provably powerful graph self-supervised learning frameworks, and hope that it would inspire both theoretical and practical future research efforts.

2 Related Work

Graph contrastive methods. Contrastive methods follow the principle of mutual information maximization [13], which typically works to maximize the correspondence or agreement between the representations of an instance (e.g., node, subgraph, or graph) in its different augmentation views. Essentially, good data augmentations and pretext tasks are the prerequisites for contrastive learning. There is a vast majority of research on graph contrastive learning [42, 34, 52, 50, 11]. To our best knowledge, graph contrastive methods are currently the most successful approaches to learning expressive representations that benefit various downstream tasks in a self-supervised fashion. However, one limitation shared by all these successful approaches is that they highly rely on the design of pretext tasks and augmentations techniques (usually summarized from many trial-and-error) to provide useful self-supervision for learning better representations [51, 16].

Graph autoencoders. GAEs in the form proposed by [18] are a family of generative models that map (encode) nodes to low-dimensional representations and reconstruct (decode) the graph. Following the autoencoding philosophy, latest approaches have demonstrated their efficacy in modeling node relationships and learning robust representations from a graph [23]. Although GAEs progressed earlier than graph contrastive approaches, they remained out of the mainstream for a long time. This is mainly due to the known limitations that GAEs suffer from. As shown in literature [42, 36, 11], GAEs tend to over-emphasize proximity information at the expense of structural information, leading to relatively poor performance on downstream tasks beyond link prediction. Despite the capability of GAEs are largely limited by the pretext task, there has been little attention paid to a better design of pretext tasks for improving the self-supervised learning scheme of GAEs.

Masked autoencoding. Masked autoencoding is one such learning task: masking a portion of input signals and attempting to predict the contents that are hidden by the mask [3]. Masked language modeling (MLM) [5, 20] is the first successful application of masked autoencoding in natural language processing. Typically, MLM is a fill-in-the-blank self-supervised learning task, where a model learns representations by predicting what a masked word should be with the context words surrounding the token. Recently, masked image modeling (MIM) [12, 48, 21] follows a similar principle to learn representations by predicting the missing parts at the pixel or patch level. MIM is gaining renewed interest from both industries and academia, leading to new state-of-the-art performance on broad downstream tasks. Despite the popularity in language and vision research, the techniques of masked autoencoding are relatively less explored in the graph domain. Until very recently, there were a few trials attempting to bridge this gap. In work concurrent with the present paper, MGAE [35] and GMAE [2] seek to apply this idea directly to graph data as a self-supervised learning paradigm, by performing masking strategies on graph structure and node attributes, respectively. However, they present only empirical results with experimental trial-and-error, which lacks further theoretical justification for a better understanding of the potential benefits of masked graph modeling.

3 Problem Formulation and Preliminaries

Problem formulation. Let $\mathcal{G} = (\mathcal{V}, \mathcal{E})$ be an undirected and unweighted graph, where $\mathcal{V} = \{v_i\}$ is a set of nodes and $\mathcal{E} \subseteq \mathcal{V} \times \mathcal{V}$ is the corresponding edges. Optionally, each node $v \in \mathcal{V}$ is associated with a d -dimensional feature vector $x_v \in \mathbb{R}^d$. The goal of most graph self-supervised learning methods, including ours, is to learn a graph encoder f_θ , which maps between the space of graph \mathcal{G} and their low-dimensional latent representations $\mathbf{Z} = \{z_i\}_{i=1}^{|\mathcal{V}|}$, such that $f_\theta(\mathcal{G}) = \mathbf{Z} \in \mathbb{R}^{|\mathcal{V}| \times d_h}$ best describes each node in \mathcal{G} , where d_h is the embedding dimension.

Background on graph neural networks. GNNs are a class of neural networks that are widely adopted as encoders for representing graph-structured data. They generally follow the canonical *message passing* scheme in which each node’s representation is computed recursively by aggregating representations (“messages”) from its immediate neighbors [17, 43, 10]. Currently, GNNs have shown great ability in modeling graph structured data and have achieved state-of-the-art results in various graph-based learning tasks [47].

Masked graph modeling (MGM). Following the masked autoencoding principle, we introduce MGM as a pretext task for graph self-supervised learning in this paper. Similar to MLM and MIM tasks in language and vision research, MGM aims to assist the model to learn more useful, transferable, and generalized representations from unlabeled graph data through masking and predicting. This

self-supervised pre-training strategy is particularly scalable when applied to GAEs since only the unmasked graph structure is processed by the network.

4 Theoretical Justification and Motivation

4.1 Revisiting graph autoencoders

GAEs, which leverage naturally occurring pairs of similar and dissimilar nodes in a graph as self-supervised signals, have shown the advantage of learning graph structures and node representations. GAEs adopt the classic encoder-decoder framework, which aims to decode from the low-dimensional representations that encode the graph by optimizing the following binary cross-entropy loss:

$$\mathcal{L}_{\text{GAEs}} = - \left(\frac{1}{|\mathcal{E}^+|} \sum_{(u,v) \in \mathcal{E}^+} \log h_\omega(z_u, z_v) + \frac{1}{|\mathcal{E}^-|} \sum_{(u',v') \in \mathcal{E}^-} \log(1 - h_\omega(z_{u'}, z_{v'})) \right) \quad (1)$$

where z is the node representation obtained from an encoder f_θ (e.g., a GNN); \mathcal{E}^+ is a set of positive edges while \mathcal{E}^- is a set of negative edges sampled from graph; Typically, $\mathcal{E}^+ = \mathcal{E}$. We denote h_ω a decoder with parameters ω .

4.2 Connecting GAEs to contrastive learning

We now provide some intuition that connects GAEs to contrastive learning from the viewpoint of the information theory. Our analysis will be based on the **homophily** assumption, i.e., the underlying semantics of nodes u and v are more likely to be the same if they are connected by an edge. We adopt the *information-maximization (infomax)* viewpoint of contrastive learning [38, 39]. Specifically, let $I(X; Y)$ be the *mutual information (MI)* between random variables X and Y taking values in \mathcal{X} and \mathcal{Y} , respectively. An important alternative characterization of MI is the following Donsker-Varadhan variational representation [27]:

$$I(X; Y) = \sup_{c: \mathcal{X} \times \mathcal{Y} \rightarrow \mathbb{R}} \mathcal{I}_c(X; Y), \quad \mathcal{I}_c(X; Y) = \mathbb{E}_{x,y \sim P_{X \times Y}} c(x, y) - \log \mathbb{E}_{x,y \sim P_X \times P_Y} (e^{c(x,y)}), \quad (2)$$

with the *critic* function c [28] ranging over the set of integrable functions taking two arguments. Under the context of GAEs, we identify X and Y with the corresponding k -hop subgraphs $\mathcal{G}^k(u)$ and $\mathcal{G}^k(v)$ of **adjacent** nodes u and v , with randomness over the generating distribution of the graph as well as the generating distributions of node features.² Denote the corresponding joint and marginal distributions as P_{UV} , P_U , and P_V , respectively. Under this formulation, we may view Eq.(1) as an empirical approximation of the following population-based objective:

$$\mathcal{I}_h^{\text{GAEs}}(U; V) = - (\mathbb{E}_{u,v \sim P_{UV}} \log h(u, v) + \mathbb{E}_{u' \sim P_U, v' \sim P_V} \log(1 - h(u', v'))). \quad (3)$$

With slight abuse of notation, we denote $I(U; V)$ as the MI between $\mathcal{G}^k(U)$ and $\mathcal{G}^k(V)$. The following lemma establishes the connection between GAE and contrastive learning over graphs:

Lemma 1. *Let $h^* \in \arg \min_{h \in \mathcal{H}} \mathcal{I}_h^{\text{GAEs}}(U; V)$. Then we have $\mathcal{I}_{h^*}(U; V) = I(U; V)$.*

Here the domain \mathcal{H} stands for the product space of all possible pairs of subgraphs. The above lemma is a direct consequence of the results in [28, 40]. Lemma 1 states that minimizing the GAE objective (1) is in population equivalent to maximizing the mutual information between the k -hop subgraphs of adjacent nodes (here k depends on the receptive fields of the encoder). Now suppose that the parameterization $h_\omega(z_u, z_v)$ is sufficiently expressive for approximating $h(u, v)$ for any $h \in \mathcal{H}$, it follows from standard results in M-estimation theory [41] that the corresponding empirical minimizer of $\mathcal{I}^{\text{GAEs}}$ converges to the maximizer of \mathcal{I} in probability. We discuss more on the expressivity and approximation issues in Appendix A.

4.3 Task related information, and redundancy of GAEs

The (asymptotic) equivalence of learned representations of GAEs and contrastive learning does not necessarily imply good performance regarding *downstream tasks*. Recent progresses on information-theoretic viewpoints of contrastive learning [38, 39] suggest that for contrastive pretraining to succeed

²The negative edge sampling process in the objective (1) is biased if negative pairs are sampled from disconnected node pairs. Since it does not affect our analysis, we discuss this further in Appendix E.

in downstream tasks, the *task irrelevant information* shall be reasonably controlled. Formally, let U, V be random variables of the two contrasting views, and T denote the target of the downstream task.³ Denote $I(U; V|T)$ as the conditional mutual information of U and V given T , we have the following simple identity which is a direct consequence of the chain rule [27].

$$\underbrace{I(U; T)}_{\text{supervised goal}} = \underbrace{I(U; V)}_{\text{self-supervised goal}} + \underbrace{I(U; T|V)}_{\text{measures task relevance}} - \underbrace{I(U; V|T)}_{\text{measures task irrelevanc}}. \quad (4)$$

The relation (4) implies that, for successful application of contrastively-pretrained representations to downstream tasks, we need both $I(U; T|V)$ and $I(U; V|T)$ to be small.⁴ A small value of $I(U; T|V)$ is a standard assumption in information-theoretic characterizations of self-supervised learning [33, 39]. The term $I(U; V|T)$ measures the *task-irrelevant* information contained in the two contrastive views U and V , regarding the downstream task T , and cannot be reduced via algorithmic designs of encoders and decoders [39]. It is therefore of interest to examine the efficacy of GAEs via assessing the task-irrelevant information, or redundancy, of the two contrasting views that use k -hop subgraphs of adjacent nodes.

Intuitively, for certain kinds of downstream task information T , we might expect $I(U; V|T)$ to be large under the GAE formulation, since k -hop subgraphs of two adjacent nodes share a (potentially) large common subgraph. From a computational point of view, the phenomenon of overlapping subgraphs may affect up to $k - 1$ layers of GNN message passing and aggregation during the encoding stage of both nodes, thereby creating a large correlation between the representations, even when the encoder has little relevance with the downstream task. To further justify the above reasoning, we give a lower bound of $I(U; V|T)$ under an independence assumption between graph topology and node features:

Proposition 1. *Suppose that the task-related information is completely reflected by the topological structure of the underlying subgraph, i.e., T is all the topological information of the underlying graph. Moreover suppose the node features are generated independently from the graph topology, with the feature of each node be (coordinate-wise) independently sampled from a zero-mean distribution supported in $[-1, 1]$ with variance γ . Let N_k be an upper bound for the size of k -hop subgraph associated with each node v , i.e., $\max_{v \in \mathcal{V}} |\mathcal{G}^k(v)|_0 \leq N_k$, we have the following lower bound of $I(U; V|T)$:*

$$I(U; V|T) \geq \frac{(\mathbb{E}[N_{uv}^k])^2}{N_k} \gamma^2, \quad (5)$$

where N_{uv}^k is the size of the overlapping subgraph of $\mathcal{G}^k(u)$ and $\mathcal{G}^k(v)$, and the expectation is taken with respect to the generating distribution of the graph and the randomness in choosing u and v .

Proposition 1 provides a quantitative characterization of task-irrelevant information of GAE. We discuss possible relaxations of the independence assumptions in Appendix A. The proof is deferred to Appendix A.

According to proposition 1, the redundancy of GAE scales almost linearly with the size of overlapping subgraphs. To design better self-supervised graph learning methods, we need a principled way to reduce the redundancy while keeping task-relevant information $I(U; T|V)$ almost intact.

5 Present Work: MaskGAE

In this section, we present the MaskGAE framework for the MGM pretext task, which is developed by taking inspiration from MLM [5] and MIM [12]. As shown in Figure 2, MaskGAE is a simple framework tailored by its *asymmetric* design, where an encoder maps the partially observed graph to a latent representation, followed by two decoders reconstructing the information of the masked structure in terms of edge and node levels. We empirically show that such an asymmetric encoder-decoder architecture helps GAEs learn generalizable and transferable representations easily. In what follows, we will give the details of the proposed MaskGAE framework from four aspects: masking strategy, encoder, decoder, and learning objective.

³Technically, T could be further relaxed to be any *sufficient statistic* of the underlying task, we adopt the more direct formulation for representation clarity

⁴When both $I(U; T|V)$ and $I(U; V|T)$ are large, the equation becomes meaningless in that T and V should be nearly independent

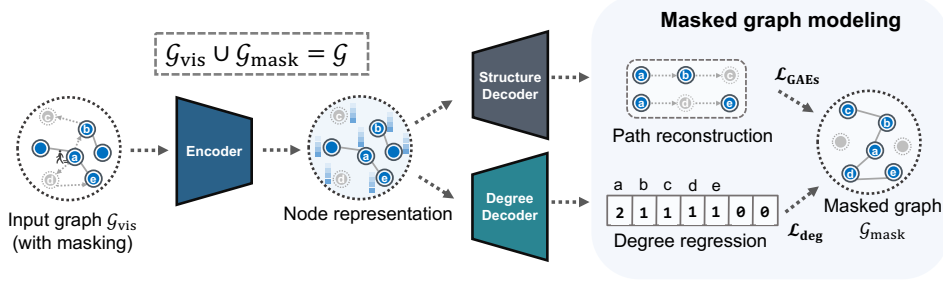


Figure 2: Overview of MaskGAE framework, performing masked graph modeling with a asymmetric encoder-decoder design. During the self-supervised learning phase, an input graph \mathcal{G}_{vis} is provided, but with some of paths (a set of adjacent edges) are masked. The goal of the model is then to learn to predict the masked edges in the graph $\mathcal{G}_{\text{mask}}$ and the degree of the associated nodes, respectively.

5.1 Masking strategy

The major difference between MaskGAE and traditional GAEs is the tailored MGM task, with masking on the input graph as a crucial operation. According to proposition 1, the redundancy of two paired subgraphs could be reduced significantly if we mask a certain portion of the edges, thereby avoiding a trivial (large) overlapping subgraph. Furthermore, previous empirical evidence [30] suggested that edge-level information is often redundant for downstream tasks like node classification, thus implicitly implies little degradation over the task-relevant information $I(U; T|V)$. Let $\mathcal{G}_{\text{mask}} = (\mathcal{E}_{\text{mask}}, \mathcal{V})$ denote the graph masked from \mathcal{G} and \mathcal{G}_{vis} the remaining visible graph. Note that $\mathcal{G}_{\text{mask}} \cup \mathcal{G}_{\text{vis}} = \mathcal{G}$. Here we introduce two masking strategies that facilitate the MGM task as follows.

Edge-wise random masking ($\mathcal{T}_{\text{edge}}$). A simple and straightforward way to form a masked graph is to sample a subset of edges $\mathcal{E}_{\text{mask}} \subseteq \mathcal{E}$ following a specific distribution, e.g., Bernoulli distribution:

$$\mathcal{E}_{\text{mask}} \sim \text{Bernoulli}(p), \quad (6)$$

where $p < 1$ is the masking rate for an input graph. Such edge masking strategy are widely used in literature [55, 52, 37]. We denote the edge-wise random masking as $\mathcal{T}_{\text{edge}}$ such that $\mathcal{G}_{\text{mask}} = \mathcal{T}_{\text{edge}}(\mathcal{G})$.

Path-wise random masking ($\mathcal{T}_{\text{path}}$). We also propose a novel structured masking strategy that takes *path* as a basic processing unit during sampling. Informally, a path in a graph is a sequence of edges which joins a sequence of adjacent nodes. Compared to simple edge masking, path-wise masking breaks the short-range connections between nodes, the model must look elsewhere for evidence to fit the structure that is masked out. Therefore, it can better exploit the structure-dependency patterns and capture the high-order proximity for more meaningful MGM tasks. For path-wise masking, we sample a set of masked edges as follows:

$$\mathcal{E}_{\text{mask}} \sim \text{RandomWalk}(\mathcal{R}, n_{\text{walk}}, l_{\text{walk}}), \quad (7)$$

where $\mathcal{R} \subseteq \mathcal{V}$ is a set of root nodes sampled from the graph, n_{walk} is the number of walks per node, and l_{walk} is the walk length. Here we sample a subset of nodes (e.g., 50%) without replacement as root nodes \mathcal{R} , following the degree distribution. Such sampling can also prevent a potential long-tailed bias existed in the graph (i.e., more masked edges are those belonging to high-degree nodes.). We perform simple random walk [26] to sample masked edges $\mathcal{E}_{\text{mask}}$, although biased random walk [9] are also applicable. We denote path-wise random masking as $\mathcal{T}_{\text{path}}$. To the best of our knowledge, our method is the first to use path-wise masking for graph self-supervised learning.

Relation with prior work. Both MaskGAE and some existing contrastive methods [55, 52, 37] apply masking on the graph. While those contrastive methods use edge masking as an augmentation to generate different structural views for contrasting, MaskGAE employs edge masking for constructing meaningful supervision signals as well as reducing the redundancy between paired subgraph views, thus facilitating the self-supervised learning scheme.

5.2 Encoder

In this work, our encoder is graph convolutional networks (GCN) [17], a well-established GNN architecture widely used in literature [42, 11]. Our framework allows various choices of the encoder

architecture, such as SAGE [10] and GAT [43], without any constraints. We opt for simplicity and adopt the commonly used GCN. Unlike traditional GAEs, our encoder only needs to process a small portion of edges during message passing, since it is applied only on a visible, unmasked subgraph. This offers an opportunity for designing an efficient and powerful encoder while alleviating the scalability problem to pretrain large GNNs.

5.3 Decoder

Structure decoder. The structure decoder is a basic design of GAEs, which by aggregating pairwise node representations as link representations to decode the graph. There are several ways to design such a decoder in literature, one can use the inner product or a neural network for decoding. We define the structure decoder h_ω with parameters ω as:

$$h_\omega(z_i, z_j) = \text{Sigmoid}(z_i^T z_j) \quad \text{or} \quad h_\omega(z_i, z_j) = \text{Sigmoid}(\text{MLP}(z_i \circ z_j)), \quad (8)$$

where MLP denotes a multilayer perceptron and \circ denotes element-wise product.

Degree decoder. We also introduce a degree decoder as an auxiliary architecture to balance proximity and structure information. As the graph structure itself has abundant supervision signals more than edge connections, we can force the model to approximate the node degree in a masked graph to facilitate the training. Specifically, the degree decoder is defined as:

$$g_\phi(z_v) = \text{MLP}(z_v), \quad (9)$$

with ϕ parameterizing the degree decoder.

5.4 Learning objective

The loss for MaskGAE has two parts: (i) **Reconstruction loss.** The reconstruction loss measures how well the model rebuilds the *masked* graph in terms of edge-reconstruction, which in a form is similar to Eq. (1), but replaces the term $\mathcal{E}^+ = \mathcal{E}_{\text{mask}}$. (ii) **Regression loss.** The regression loss measures how closely the prediction of node degree match to the original one in the masked graph. We compute the mean squared error (MSE) between the approximated and original degree in terms of node level:

$$\mathcal{L}_{\text{deg}} = \frac{1}{|\mathcal{V}|} \sum_{v \in \mathcal{V}} \|g_\phi(z_v) - \text{deg}_{\text{mask}}(v)\|_F^2, \quad (10)$$

where deg_{mask} denotes the node degree in the masked graph $\mathcal{G}_{\text{mask}}$. Essentially, $\mathcal{L}_{\text{deg}}(\cdot)$ can work as a regularizer for the encoder to learn more generalizable representations. Thus, the overall objective to be minimized when training the model is:

$$\mathcal{L} = \mathcal{L}_{\text{GAEs}} + \alpha \mathcal{L}_{\text{deg}}, \quad (11)$$

where α is a non-negative hyperparameter trading off two terms. Note that we compute the loss only on masked graph, similar to MAE [12]. The pseudo-code of MaskGAE is provided in Appendix C.

6 Experiments

In this section, we compare MaskGAE with state-of-the-art methods. According to different masking strategies, we have $\text{MaskGAE}_{\text{edge}}$ and $\text{MaskGAE}_{\text{path}}$, denoting MaskGAE with edge-wise and path-wise masking strategies, respectively. We consider two fundamental tasks associated with graph representation learning: link prediction and node classification. In all tables and datasets, we report averaged results along with the standard deviation computed over 10 different runs. Appendix D reports further details on the experiments and reproducibility.

6.1 Performance comparison on link prediction

As GAEs, including ours, are initially designed for graph reconstruction, the trained model can easily perform link prediction task without additional fine-tuning. For fair comparison, we only compare MaskGAE with following methods, including (V)GAE [18], AR(V)GA [23], SAGE [10], and MGAE [35], which are trained in an end-to-end fashion to perform link prediction. Following a

Table 1: Link prediction results (%) on three citation networks. In each column, the **boldfaced** score denotes the best result and the underlined score represents the second-best result.

	Cora		CiteSeer		PubMed	
	AUC	AP	AUC	AP	AUC	AP
GAE	91.09 \pm 0.01	92.83 \pm 0.03	90.52 \pm 0.04	91.68 \pm 0.05	96.40 \pm 0.01	96.50 \pm 0.02
VGAE	91.40 \pm 0.01	92.60 \pm 0.01	90.80 \pm 0.02	92.00 \pm 0.02	94.40 \pm 0.02	94.70 \pm 0.02
ARGA	92.40 \pm 0.00	93.23 \pm 0.00	91.94 \pm 0.00	93.03 \pm 0.00	96.81 \pm 0.00	97.11 \pm 0.00
ARVGA	92.40 \pm 0.00	92.60 \pm 0.00	92.40 \pm 0.00	93.00 \pm 0.00	96.50 \pm 0.00	96.80 \pm 0.00
SAGE	86.33 \pm 1.06	88.24 \pm 0.87	85.65 \pm 2.56	87.90 \pm 2.54	89.22 \pm 0.87	89.44 \pm 0.82
MGAE	95.05 \pm 0.76	94.50 \pm 0.86	94.85 \pm 0.49	94.68 \pm 0.34	98.45 \pm 0.03	98.22 \pm 0.05
MaskGAE _{edge}	<u>96.49\pm0.32</u>	<u>96.10\pm0.35</u>	98.00\pm0.23	98.25\pm0.16	<u>98.77\pm0.02</u>	<u>98.62\pm0.05</u>
MaskGAE _{path}	96.66\pm0.17	96.29\pm0.23	<u>97.95\pm0.10</u>	<u>98.12\pm0.10</u>	99.06\pm0.05	98.99\pm0.06

standard manner of learning-based link prediction [18], we conduct experiments on Cora, CiteSeer and PubMed, removing 5% edges for validation and 10% edges for test.

We report AUC score and average precision (AP). The results of baselines are quoted from [23, 35]. As shown in Table 1, both variants of MaskGAE achieve the leading performance over all compared algorithms regarding all evaluation metrics. Specifically, MaskGAE_{edge} and MaskGAE_{path} significantly outperform vanilla GAE on three datasets with an increase in AUCs score and AP score by 5% on average, demonstrating the effectiveness of the proposed MaskGAE framework. We believe the result comes from the benefits of the MGM paradigm. On one hand, MGM helps self-supervised learning of GAEs by reducing the redundancy of contrastive views. On the other hand, MGM naturally eliminates the discrepancy between pre-training and downstream tasks, as the model is required to predict a portion of edges that are “invisible” given partial visible structure in both stages. In this regard, MGM help improve the performance of GAEs in modeling the graph structure and outperform the leading baselines.

6.2 Performance comparison on node classification

We also perform node classification under the self-supervised learning setting to validate the effectiveness of learned representations. The model is trained on a partially observed graph in a self-supervised way, with the same setting as the link prediction task. We compare against baselines belonging to the three categories: (i) **generative learning** algorithms, including (V)GAE [18] and AR(V)GA [23]; (ii) **contrastive learning** algorithms, including DGI [42], GMI [25], GRACE [55], GCA [56], MV-GRL [11], BGRL [37], SUGRL [22], CCA-SSG [53]. (iii) **supervised or semi-supervised** methods, including MLP, GCN [17] and GAT [43]. Both (i) and (ii) are self-supervised methods. We closely follow the linear evaluation scheme as introduced in [42, 53] and report the classification accuracy on all datasets. For further details, please refer to Appendix D.

The results are presented in Table 2. For self-supervised approaches, we can see that the contrastive methods generally outperform generative methods (GAEs), which verify the effectiveness of contrastive learning. This also highlights the fact that the learned representations by GAEs are not task-agnostic, which cannot generalize to other downstream tasks beyond link prediction. In contrast, both variants of MaskGAE outperform or match the best contrastive approaches across all datasets. Even compared with the supervised ones, MaskGAE outperforms all the baselines. The results clearly demonstrate the effectiveness of the proposed MaskGAE framework and validate our claims.

It is observed that MaskGAE exhibits good computational scaling and downstream performance on large datasets arXiv and MAG. This may be due to the fact that only a small portion of unmasked edges are processed by the encoder during training and thus benefiting the scalability. Note that CCA-SSG has a poor performance on arXiv and MAG since it is essentially a dimension-reduction method, where the ideal embedding dimension ought to be smaller than input one [53].

We also see that both variants of MaskGAE using masking strategies achieve the leading performance, while MaskGAE_{path} achieves relatively better performance than MaskGAE_{edge} in most cases. It is probably because that path-wise masking enforces a model to predict a set of edges that are locally correlated, thus creating a task that cannot be easily solved by extrapolation from visible

Table 2: Node classification accuracy (%) on seven benchmark datasets. In each column, the **boldfaced** score denotes the best result and the underlined score represents the second-best result.

	Cora	CiteSeer	PubMed	Photo	Computer	arXiv	MAG
MLP	47.90 \pm 0.40	49.30 \pm 0.30	69.10 \pm 0.20	78.50 \pm 0.20	73.80 \pm 0.10	56.30 \pm 0.30	22.10 \pm 0.30
GCN	81.50 \pm 0.20	70.30 \pm 0.40	79.00 \pm 0.50	92.42 \pm 0.22	86.51 \pm 0.54	70.40 \pm 0.30	30.10 \pm 0.30
GAT	83.00 \pm 0.70	72.50 \pm 0.70	79.00 \pm 0.30	92.56 \pm 0.35	86.93 \pm 0.29	70.60 \pm 0.30	30.50 \pm 0.30
GAE	74.90 \pm 0.40	65.60 \pm 0.50	74.20 \pm 0.30	91.00 \pm 0.10	85.10 \pm 0.40	63.60 \pm 0.50	27.10 \pm 0.30
VGAE	76.30 \pm 0.20	66.80 \pm 0.20	75.80 \pm 0.40	91.50 \pm 0.20	85.80 \pm 0.30	64.80 \pm 0.20	27.90 \pm 0.20
ARGA	77.95 \pm 0.70	64.44 \pm 1.19	80.44 \pm 0.74	91.82 \pm 0.08	85.86 \pm 0.11	67.34 \pm 0.09	28.36 \pm 0.12
ARVGA	79.50 \pm 1.01	66.03 \pm 0.65	81.51 \pm 1.00	91.51 \pm 0.09	86.02 \pm 0.11	67.43 \pm 0.08	28.32 \pm 0.18
DGI	82.30 \pm 0.60	71.80 \pm 0.70	76.80 \pm 0.60	91.61 \pm 0.22	83.95 \pm 0.47	65.10 \pm 0.40	31.40 \pm 0.30
GMI	83.00 \pm 0.30	72.40 \pm 0.10	79.90 \pm 0.20	90.68 \pm 0.17	82.21 \pm 0.31	68.20 \pm 0.20	29.50 \pm 0.10
GRACE	81.90 \pm 0.40	71.20 \pm 0.50	80.60 \pm 0.40	92.15 \pm 0.24	86.25 \pm 0.25	68.70 \pm 0.40	31.50 \pm 0.30
GCA	81.80 \pm 0.20	71.90 \pm 0.40	81.00 \pm 0.30	92.53 \pm 0.16	87.85 \pm 0.31	68.20 \pm 0.20	31.40 \pm 0.30
MVGRL	82.90 \pm 0.30	72.60 \pm 0.40	80.10 \pm 0.70	91.70 \pm 0.10	86.90 \pm 0.10	68.10 \pm 0.10	31.60 \pm 0.40
BGRL	82.86 \pm 0.49	71.41 \pm 0.92	82.05 \pm 0.85	93.17 \pm 0.30	90.34 \pm 0.19	71.64 \pm 0.12	31.11 \pm 0.11
SUGRL	83.40 \pm 0.50	73.00 \pm 0.40	81.90 \pm 0.30	<u>93.20</u> \pm 0.40	88.90 \pm 0.20	69.30 \pm 0.20	32.40 \pm 0.10
CCA-SSG	83.59 \pm 0.73	<u>73.36</u> \pm 0.72	80.81 \pm 0.38	93.14 \pm 0.14	88.74 \pm 0.28	52.55 \pm 0.10	23.39 \pm 0.63
MaskGAE _{edge}	83.61 \pm 0.14	72.12 \pm 0.16	82.69 \pm 0.31	93.21 \pm 0.13	89.39 \pm 0.13	70.11 \pm 0.36	<u>32.42</u> \pm 0.38
MaskGAE _{path}	84.05 \pm 0.18	73.49 \pm 0.59	83.06 \pm 0.22	93.09 \pm 0.06	<u>89.51</u> \pm 0.08	<u>70.73</u> \pm 0.30	32.79 \pm 0.26

graph structure. In this regard, the learned representations are more robust and generalizable, leading to better performance on downstream tasks. This implies that path-wise masking might be a more promising masking strategy for the MGM task. We also conduct ablation study on different components of MaskGAE. We leave the results and discussions in Appendix D.2.

7 Conclusion

In this work, we make the first investigation on masked graph modeling (MGM) and present MaskGAE, a theoretically grounded self-supervised learning framework that takes MGM as a principled pretext task. Our work is theoretically motivated with the following justifications: (i) GAEs are essentially contrastive learning that maximizes the mutual information between paired subgraph views associated with a linked edge, and (ii) MGM can benefit the mutual information maximization since masking significantly reduce the redundancy between two subgraph views. In particular, we also propose a path-wise masking strategy to facilitate the MGM task. In our experiments, MaskGAE exhibits significantly improved performances over GAEs and performs on par with or better than strong baselines on link prediction and node classification benchmarks.

References

- [1] M. I. Belghazi, A. Baratin, S. Rajeshwar, S. Ozair, Y. Bengio, A. Courville, and D. Hjelm. Mutual information neural estimation. In *ICML*, volume 80, pages 531–540. PMLR, 10–15 Jul 2018.
- [2] H. Chen, S. Zhang, and G. Xu. Graph masked autoencoder. *CoRR*, abs/2202.08391, 2022.
- [3] Z. Chen, D. Agarwal, K. Aggarwal, W. Safta, M. M. Balan, V. Sethuraman, and K. Brown. Masked image modeling advances 3d medical image analysis. *arXiv preprint arXiv: 2204.11716*, 2022.
- [4] D. Clevert, T. Unterthiner, and S. Hochreiter. Fast and accurate deep network learning by exponential linear units (elus). In *ICLR (Poster)*, 2016.
- [5] J. Devlin, M. Chang, K. Lee, and K. Toutanova. BERT: pre-training of deep bidirectional transformers for language understanding. In *NAACL-HLT (1)*, pages 4171–4186. Association for Computational Linguistics, 2019.
- [6] M. Fey and J. E. Lenssen. Fast graph representation learning with PyTorch Geometric. In *ICLR Workshop on Representation Learning on Graphs and Manifolds*, 2019.

- [7] V. Garg, S. Jegelka, and T. Jaakkola. Generalization and representational limits of graph neural networks. In *ICML*, pages 3419–3430. PMLR, 2020.
- [8] A. Goldenberg, A. X. Zheng, S. E. Fienberg, E. M. Airolidi, et al. A survey of statistical network models. *Foundations and Trends® in Machine Learning*, 2(2):129–233, 2010.
- [9] A. Grover and J. Leskovec. node2vec: Scalable feature learning for networks. In *KDD*, pages 855–864, 2016.
- [10] W. Hamilton, Z. Ying, and J. Leskovec. Inductive representation learning on large graphs. In *NeurIPS*, pages 1024–1034, 2017.
- [11] K. Hassani and A. H. K. Ahmadi. Contrastive multi-view representation learning on graphs. In *ICML*, volume 119, pages 4116–4126. PMLR, 2020.
- [12] K. He, X. Chen, S. Xie, Y. Li, P. Dollár, and R. B. Girshick. Masked autoencoders are scalable vision learners. *CoRR*, abs/2111.06377, 2021.
- [13] R. D. Hjelm, A. Fedorov, S. Lavoie-Marchildon, K. Grewal, P. Bachman, A. Trischler, and Y. Bengio. Learning deep representations by mutual information estimation and maximization. In *ICLR*. OpenReview.net, 2019.
- [14] W. Hu, M. Fey, M. Zitnik, Y. Dong, H. Ren, B. Liu, M. Catasta, and J. Leskovec. Open graph benchmark: Datasets for machine learning on graphs. *arXiv preprint arXiv:2005.00687*, 2020.
- [15] S. Ioffe and C. Szegedy. Batch normalization: Accelerating deep network training by reducing internal covariate shift. In *ICML*, volume 37 of *JMLR Workshop and Conference Proceedings*, pages 448–456. JMLR.org, 2015.
- [16] W. Jin, X. Liu, X. Zhao, Y. Ma, N. Shah, and J. Tang. Automated self-supervised learning for graphs. In *International Conference on Learning Representations*, 2022.
- [17] T. N. Kipf and M. Welling. Semi-supervised classification with graph convolutional networks. *arXiv preprint arXiv:1609.02907*, 2016.
- [18] T. N. Kipf and M. Welling. Variational graph auto-encoders. *CoRR*, abs/1611.07308, 2016.
- [19] N. Lee, J. Lee, and C. Park. Augmentation-free self-supervised learning on graphs. 2022.
- [20] Y. Liu, M. Ott, N. Goyal, J. Du, M. Joshi, D. Chen, O. Levy, M. Lewis, L. Zettlemoyer, and V. Stoyanov. Roberta: A robustly optimized BERT pretraining approach. *CoRR*, abs/1907.11692, 2019.
- [21] A. Mahmoud, C. Mathilde, M. Ishan, B. Piotr, B. Florian, V. Pascal, J. Armand, R. Michael, and B. Nicolas. Masked siamese networks for label-efficient learning. *arXiv preprint arXiv:2204.07141*, 2022.
- [22] Y. Mo, L. Peng, J. Xu, X. Shi, and X. Zhu. Simple unsupervised graph representation learning. *AAAI*, 2022.
- [23] S. Pan, R. Hu, G. Long, J. Jiang, L. Yao, and C. Zhang. Adversarially regularized graph autoencoder for graph embedding. In *IJCAI*, pages 2609–2615. ijcai.org, 2018.
- [24] A. Paszke, S. Gross, F. Massa, A. Lerer, J. Bradbury, G. Chanan, T. Killeen, Z. Lin, N. Gimelshein, L. Antiga, A. Desmaison, A. Köpf, E. Z. Yang, Z. DeVito, M. Raison, A. Tejani, S. Chilamkurthy, B. Steiner, L. Fang, J. Bai, and S. Chintala. Pytorch: An imperative style, high-performance deep learning library. In *NeurIPS*, pages 8024–8035, 2019.
- [25] Z. Peng, W. Huang, M. Luo, Q. Zheng, Y. Rong, T. Xu, and J. Huang. Graph representation learning via graphical mutual information maximization. In *WWW*, pages 259–270. ACM / IW3C2, 2020.
- [26] B. Perozzi, R. Al-Rfou, and S. Skiena. Deepwalk: online learning of social representations. In *KDD*, pages 701–710. ACM, 2014.
- [27] Y. Polyanskiy and Y. Wu. Lecture notes on information theory. *Lecture Notes for ECE563 (UIUC) and*, 6(2012-2016):7, 2014.
- [28] B. Poole, S. Ozair, A. Van Den Oord, A. Alemi, and G. Tucker. On variational bounds of mutual information. In K. Chaudhuri and R. Salakhutdinov, editors, *ICML*, volume 97 of *Proceedings of Machine Learning Research*, pages 5171–5180. PMLR, 09–15 Jun 2019.
- [29] Y. Rong, Y. Bian, T. Xu, W. Xie, Y. Wei, W. Huang, and J. Huang. Self-supervised graph transformer on large-scale molecular data. *NeurIPS*, 33:12559–12571, 2020.

- [30] Y. Rong, W. Huang, T. Xu, and J. Huang. Dropedge: Towards deep graph convolutional networks on node classification. In *ICLR*. OpenReview.net, 2020.
- [31] P. Sen, G. Namata, M. Bilgic, L. Getoor, B. Galligher, and T. Eliassi-Rad. Collective classification in network data. *AI magazine*, 29(3):93–93, 2008.
- [32] O. Shchur, M. Mumme, A. Bojchevski, and S. Günnemann. Pitfalls of graph neural network evaluation. *Relational Representation Learning Workshop, NeurIPS*, 2018.
- [33] K. Sridharan and S. M. Kakade. An information theoretic framework for multi-view learning. In *Conference on Learning Theory*. PMLR, 2008.
- [34] S. Suresh, P. Li, C. Hao, and J. Neville. Adversarial graph augmentation to improve graph contrastive learning. In *NeurIPS*, pages 15920–15933, 2021.
- [35] Q. Tan, N. Liu, X. Huang, R. Chen, S. Choi, and X. Hu. MGAE: masked autoencoders for self-supervised learning on graphs. *CoRR*, abs/2201.02534, 2022.
- [36] M. Tang, P. Li, and C. Yang. Graph auto-encoder via neighborhood wasserstein reconstruction. In *International Conference on Learning Representations*, 2022.
- [37] S. Thakoor, C. Tallec, M. G. Azar, R. Munos, P. Veličković, and M. Valko. Bootstrapped representation learning on graphs. In *ICLR 2021 Workshop on Geometrical and Topological Representation Learning*, 2021.
- [38] Y. Tian, C. Sun, B. Poole, D. Krishnan, C. Schmid, and P. Isola. What makes for good views for contrastive learning? In H. Larochelle, M. Ranzato, R. Hadsell, M. Balcan, and H. Lin, editors, *NeurIPS*, volume 33, pages 6827–6839. Curran Associates, Inc., 2020.
- [39] Y.-H. H. Tsai, Y. Wu, R. Salakhutdinov, and L.-P. Morency. Self-supervised learning from a multi-view perspective. In *ICLR*, 2021.
- [40] Y.-H. H. Tsai, H. Zhao, M. Yamada, L.-P. Morency, and R. R. Salakhutdinov. Neural methods for point-wise dependency estimation. *NeurIPS*, 33:62–72, 2020.
- [41] A. W. Van der Vaart. *Asymptotic statistics*, volume 3. Cambridge university press, 2000.
- [42] P. Velićković, W. Fedus, W. L. Hamilton, P. Liò, Y. Bengio, and R. D. Hjelm. Deep graph infomax. *ICLR (Poster)*, 2(3):4, 2019.
- [43] P. Velićković, G. Cucurull, A. Casanova, A. Romero, P. Liò, and Y. Bengio. Graph attention networks. In *ICLR*, 2018.
- [44] M. J. Wainwright. *High-dimensional statistics: A non-asymptotic viewpoint*, volume 48. Cambridge University Press, 2019.
- [45] M. J. Wainwright, M. I. Jordan, et al. Graphical models, exponential families, and variational inference. *Foundations and Trends® in Machine Learning*, 1(1–2):1–305, 2008.
- [46] J. Wang, S. Zhang, Y. Xiao, and R. Song. A review on graph neural network methods in financial applications. *arXiv preprint arXiv:2111.15367*, 2021.
- [47] L. Wu, H. Lin, C. Tan, Z. Gao, and S. Z. Li. Self-supervised learning on graphs: Contrastive, generative, or predictive. *TKDE*, 2021.
- [48] Z. Xie, Z. Zhang, Y. Cao, Y. Lin, J. Bao, Z. Yao, Q. Dai, and H. Hu. Simmim: A simple framework for masked image modeling. *CoRR*, abs/2111.09886, 2021.
- [49] A. Xu and M. Raginsky. Information-theoretic analysis of generalization capability of learning algorithms. *Advances in Neural Information Processing Systems*, 30, 2017.
- [50] D. Xu, W. Cheng, D. Luo, H. Chen, and X. Zhang. Infogcl: Information-aware graph contrastive learning. In *NeurIPS*, pages 30414–30425, 2021.
- [51] Y. You, T. Chen, Y. Shen, and Z. Wang. Graph contrastive learning automated. In *ICML*, volume 139 of *Proceedings of Machine Learning Research*, pages 12121–12132. PMLR, 2021.
- [52] Y. You, T. Chen, Y. Sui, T. Chen, Z. Wang, and Y. Shen. Graph contrastive learning with augmentations. In *NeurIPS*, 2020.
- [53] H. Zhang, Q. Wu, J. Yan, D. Wipf, and P. S. Yu. From canonical correlation analysis to self-supervised graph neural networks. In *NeurIPS*, 2021.
- [54] C. Zhao, S. Liu, F. Huang, S. Liu, and W. Zhang. CSGNN: contrastive self-supervised graph neural network for molecular interaction prediction. In *IJCAI*, pages 3756–3763. ijcai.org, 2021.

- [55] Y. Zhu, Y. Xu, F. Yu, Q. Liu, S. Wu, and L. Wang. Deep Graph Contrastive Representation Learning. In *ICML Workshop on Graph Representation Learning and Beyond*, 2020.
- [56] Y. Zhu, Y. Xu, F. Yu, Q. Liu, S. Wu, and L. Wang. Graph contrastive learning with adaptive augmentation. In *WWW*, pages 2069–2080. ACM / IW3C2, 2021.

A Proofs

The key ingredient of the proof of proposition 1 is the following lemma, which is a conditional version of [49, Lemma 1]:

Lemma 2. Consider three random variables X, Y and T . Denote $P_{XY|T}$ as the joint distribution of X and Y given T , and $P_{X|T}$ and $P_{Y|T}$ as conditional distribution of X and Y given T , respectively. Let $q : \mathcal{X} \times \mathcal{Y} \times \mathcal{T} \mapsto \mathbb{R}$ be a function such that for any given $t \in \mathcal{T}$, q is σ -subgaussian in the product of distributions $P_{X|T=t} \times P_{Y|T=t}$, i.e.,

$$\log \mathbb{E}_{x \sim P_{X|T=t}, y \sim P_{Y|T=t}} \left[e^{\lambda(q(x, y, t))} \right] - \lambda \mathbb{E}_{x \sim P_{X|T=t}, y \sim P_{Y|T=t}} [q(x, y, t)] \leq \frac{\lambda^2 \sigma^2}{2}, \forall \lambda. \quad (12)$$

Then we have the following lower bound on the conditional MI $I(X; Y|T)$:

$$\sigma \sqrt{2I(X; Y|T)} \geq \left| \mathbb{E}_T \mathbb{E}_{x, y \sim P_{XY|T=t}} [q(x, y, t)] - \mathbb{E}_{\bar{x} \sim P_{X|T=t}, \bar{y} \sim P_{Y|T=t}} [q(\bar{x}, \bar{y}, t)] \right|. \quad (13)$$

Proof of proposition 1. We show the proposition with the feature dimension $d = 1$, and extending to general finite feature dimensions is straightforward. By the conditional version of data processing inequality [27], for any **subgraph encoding map** \mathcal{M}_k that maps k -hop subgraphs of any node v into real vectors, we have:

$$I(U; V|T) \geq I(\mathcal{M}_k(\mathcal{G}^k(u)); \mathcal{M}_k(\mathcal{G}^k(v))|T). \quad (14)$$

For notational simplicity we let $m^k(v) = \mathcal{M}_k(\mathcal{G}^k(v))$ for $\forall v \in \mathcal{V}$. Now it suffices to bound $I(U; V|T)$ under a certain encoding map, which we construct as follows: Conditional on the topological information of the underlying graph \mathcal{G} with size $N = |\mathcal{G}|$, we associate each node v with an index $\text{id}(v)$ that corresponds to its order in the topological traversal of the graph. Then $m^k(v)$ is a sparse vector of length N , with nonzero positions defined as:

$$m^k(v)[\text{id}(u)] = x(u), \forall u \in \mathcal{G}^k(v), \quad (15)$$

where we use $x[k]$ to denote the k -th element of a vector x . To bound $I(m^k(U); m^k(V)|T)$ from below, we use lemma 2 via choosing q to be the euclidean inner product:

$$q(m^k(u), m^k(v), t) = \langle m^k(u), m^k(v) \rangle = \sum_{i=1}^N m^k(u)[i] m^k(v)[i] \quad (16)$$

First we assess the subgaussian property of q . Note that each summand in Eq.(16) is a product of two independent zero-mean random variables with range $[-1, 1]$, it follows from standard results of subgaussian random variables [44] that each summand is subgaussian with coefficient 1. Since Eq.(16) has at most N_k nonzero summands. It follows by the property of subgaussian random variables implies that q is subgaussian with $\sigma \leq \sqrt{N_k}, \forall t \in \mathcal{T}$. Next we investigate the expectation of q under different distributions, note that given the topological structure, the randomness is only with respect to the generating distribution of node features. It follows from the independence of node features and the zero-mean assumption, that

$$\mathbb{E}_{\bar{x} \sim P_{X|T=t}, \bar{y} \sim P_{Y|T=t}} q(\bar{x}, \bar{y}, t) = 0, \forall t \in \mathcal{T}. \quad (17)$$

Similarly, we have

$$\mathbb{E}_{x, y \sim P_{XY|T=t}} f(x, y, t) = \gamma N_{uv}^k, \forall t \in \mathcal{T}, \quad (18)$$

since the rest $N - N_{uv}^k$ pairs are orthogonal. Applying lemma 2 we get the desired result:

$$I(U; V|T) \geq I(m^k(U); m^k(V)|T) \geq \frac{(\mathbb{E}[N_{uv}^k])^2}{N_k} \gamma^2 \quad (19)$$

□

Proof of lemma 2. The proof goes along similar arguments in [49], with slight modifications in the conditional case. First by the Donsker-Varadhan variational representation of conditional mutual information:

$$I(X; Y|T) \geq \mathbb{E}_T \left[\mathbb{E}_{x, y \sim P_{XY|T=t}} \lambda q(x, y, t) - \log \mathbb{E}_{\bar{x} \sim P_{X|T=t}, \bar{y} \sim P_{Y|T=t}} \left(e^{\lambda q(\bar{x}, \bar{y}, t)} \right) \right] \quad (20)$$

By the required subgaussian assumption we have

$$I(X; Y|T) \geq \mathbb{E}_T \left[\lambda \mathbb{E}_{x, y \sim XY|T=t} q(x, y, t) - \lambda \mathbb{E}_{\bar{x} \sim P_X|T=t, \bar{y} \sim P_Y|T=t} q(\bar{x}, \bar{y}, t) \right] - \frac{\lambda^2 \sigma^2}{2} \quad (21)$$

Viewing the equation (21) as a nonnegative parabola and set its discriminant to be nonpositive yield the result. \square

A.1 On approximating $I(U; V)$

Recall that $z_v = f_\theta(\mathcal{G})[v]$, for clarification of parameter dependence, we write $z_v := f_\theta(v)$ without further understandings. Minimization of the GAE loss (1) is therefore stated as:

$$\omega^*, \theta^* \in \arg \min_{\omega \in \Omega, \theta \in \Theta} \mathcal{L}_{\text{GAEs}}(\omega, \theta) \quad (22)$$

First we consider the ideal situation that the parameter space $\Omega \times \Theta$ is sufficiently large so that there exists $\theta_0 \in \Theta$ and $\omega_0 \in \Omega$ such that

$$h_{\omega_0}(f_{\theta_0}(u), f_{\theta_0}(v)) = \log \frac{p(u, v)}{p(u)p(v)}, \forall u, v \quad (23)$$

Now we use the fact that the pointwise dependency $\log \frac{p(u, v)}{p(u)p(v)}$ [40] is both the optimizer of the Donsker-Varadhan variational objective [27] and the objective (3) [40]. Standard results on M-estimation [41, Theorem 5.7] suggest that, if we are allowed to sample from the generating distribution of \mathcal{G} and get arbitrary number of samples (we assume the satisfaction of empirical process conditions as in the discussion of [1]), we have $w^* \xrightarrow{P} \omega_0$ and $\theta^* \xrightarrow{P} \theta_0$ with the number of samples goes to infinity. In practice, the actual parameterization may not achieve the ideal property (23) using GNN as encoders: standard results in expressivity of locally unordered message passing [7] indicates that there exists certain pairs of subgraphs that cannot be distinguished by most of the off-shelf GNN models. Consequently the condition (23) is violated. Nonetheless, we may view the problem (22) as being composed of two subproblems:

$$\omega^* = \omega^*(\theta^*) \in \arg \min_{\omega \in \Omega} \mathcal{L}_{\text{GAEs}}(\omega, \theta^*), \quad (24)$$

$$\theta^* \in \arg \min_{\theta \in \Theta} \min_{\omega \in \Omega} \mathcal{L}_{\text{GAEs}}(\omega, \theta), \quad (25)$$

with the inner problem satisfies that for any given $\theta \in \Theta$,

$$\mathcal{I}_{h^*(\theta)}(f_\theta(U); f_\theta(V)) = I(f_\theta(U); f_\theta(V)). \quad (26)$$

Here the function approximation is possible if ω is parameterized as an MLP with sufficient capacity.

A.2 Discussions on proposition 1

There appears two issues regarding the statement of proposition 1:

On the downstream target T . In the original statement, T is set to be the topological information of the underlying graph. This appears to be somewhat necessary since graph learning shall exploit topological structure. A possible relaxation could be to let \bar{T} be *local topological information* considering only $\mathcal{G}^k(v)$ for any $v \in \mathcal{V}$. Such relaxation does not affect the result of proposition 1 much since we just need to restrict the analysis to certain subgraphs. The situation becomes more complicated if we allow T to be a hybrid of feature and topological information, i.e., there are some additional randomness not captured by T regarding both feature and topology. We left corresponding explorations to future research.

On the independence between X and T . The independence assumption might not be appropriate for certain types of generating mechanisms. For example, in many popular probabilistic models of graph-like random graph models [8] and Markov random fields [45], if we treat node features as random samples from such graph models, conditional on the graph structure, node features are correlated according to whether a path exists between the underlying nodes. Incorporating dependence

in proposition 1 will result in trivial bounds in the worst case: via investigating the proof, since sums of correlated subgaussian random variables are subgaussian with a potentially much larger coefficient (N_k instead of $\sqrt{N_k}$), resulting in a lower bound no greater than the variance of a single node. This trivial lower bound, however, cannot be improved under general dependence of node features. Consider the following extreme case where the underlying graph is complete, and adjacent nodes are perfectly correlated, i.e., all node features are the same with probability one. In this extreme case, the randomness of the entire graph boils down to the randomness of any single node in the graph, and the mutual information of any two subgraphs will thus not exceeds the entropy of a single node, with is proportional to the variance of the node if the node feature is a zero-mean random variable. A more careful examination of $I(U; V|T)$ under some specified dependence structure between nodes is therefore valuable, and we left it to future studies.

B Subgraph Overlapping

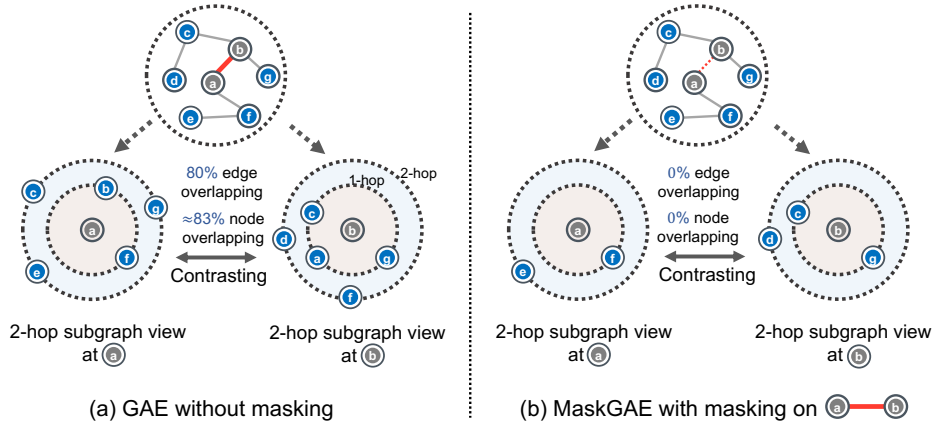


Figure 3: Illustrative examples of the benefits of the masking-and-predicting scheme. Masking on the positive edge helps the contrastive scheme, as it significantly reduces the redundancy of two paired subgraph views.

Illustrative example. We first showcase how masking assists the self-supervised learning of GAEs. As shown in Figure 3(a), we showcase how vanilla GAE fails to learn better representations. Consider an edge $a \leftrightarrow b$ as a positive example, the subgraphs centered at a and b naturally form two contrastive views. However, there exists a large overlapping in terms of nodes and edges between the paired subgraph views, which hinders the contrastive learning of GAE. In contrast, MaskGAE with masking on the edge $a \leftrightarrow b$ can avoid a trivial (large) overlapping subgraph and thus benefit the contrastive scheme of GAEs (see Figure 3(b)).

Table 3: Statistics of subgraph overlapping (%) on three citation networks.

		Cora			CiteSeer			PubMed		
		w/o mask	$\mathcal{T}_{\text{edge}}$	$\mathcal{T}_{\text{path}}$	w/o mask	$\mathcal{T}_{\text{edge}}$	$\mathcal{T}_{\text{path}}$	w/o mask	$\mathcal{T}_{\text{edge}}$	$\mathcal{T}_{\text{path}}$
$k = 2$	$\mathcal{O}_{\text{node}}$	63.43	31.74	26.97	71.93	33.01	17.05	47.09	23.83	21.81
	$\mathcal{O}_{\text{edge}}$	62.17	29.57	24.90	70.97	30.94	15.66	46.43	22.09	20.54
$k = 3$	$\mathcal{O}_{\text{node}}$	69.11	39.66	33.56	78.90	41.07	22.68	56.28	33.52	32.68
	$\mathcal{O}_{\text{edge}}$	68.68	38.78	32.84	78.61	40.66	22.34	58.06	33.65	33.32

Subgraph overlapping w/ and w/o masking. We also compute the average overlapping of all paired subgraphs in terms of node and edge levels, denoting as $\mathcal{O}_{\text{node}}$ and $\mathcal{O}_{\text{edge}}$, respectively. The

computation of both metrics are as follows:

$$\begin{aligned}\mathcal{O}_{\text{node}} &= \frac{1}{|\mathcal{E}^+|} \sum_{(u,v) \in \mathcal{E}^+} 0.5 \times \left(\frac{|\mathcal{V}^k(u) \cap \mathcal{V}^k(v)|}{|\mathcal{V}^k(u)|} + \frac{|\mathcal{V}^k(u) \cap \mathcal{V}^k(v)|}{|\mathcal{V}^k(v)|} \right), \\ \mathcal{O}_{\text{edge}} &= \frac{1}{|\mathcal{E}^+|} \sum_{(u,v) \in \mathcal{E}^+} 0.5 \times \left(\frac{|\mathcal{E}^k(u) \cap \mathcal{E}^k(v)|}{|\mathcal{E}^k(u)|} + \frac{|\mathcal{E}^k(u) \cap \mathcal{E}^k(v)|}{|\mathcal{E}^k(v)|} \right),\end{aligned}\tag{27}$$

where $\mathcal{V}^k(v)$ and $\mathcal{E}^k(v)$ represent the node set and edge set w.r.t. the k -hop subgraph at node v , respectively. Here we compute only on the positive edges, i.e., $\mathcal{E}^+ = \mathcal{E}$ (w/o masking) or $\mathcal{E}^+ = \mathcal{E}_{\text{mask}}$ (w/ masking). Table 3 presents the overlapping results on three citation graphs in terms of different hops (k) and masking strategies ($\mathcal{T}_{\text{edge}}$ and $\mathcal{T}_{\text{path}}$). As shown, both $\mathcal{O}_{\text{node}}$ and $\mathcal{O}_{\text{edge}}$ are significantly reduced with our masking strategies. Notably, $\mathcal{T}_{\text{path}}$ exhibits better capability than $\mathcal{T}_{\text{edge}}$ in reducing the subgraph overlapping, as evidenced by consistently lower $\mathcal{O}_{\text{node}}$ and $\mathcal{O}_{\text{edge}}$ on three datasets. Overall, the result demonstrates the superiority of path-wise masking strategy.

C Algorithm

To help better understand the proposed framework, we provide the detailed algorithm and PyTorch-style pseudocode for training MaskGAE in Algorithm 1 and Algorithm 2, respectively.

Algorithm 1 Masked Graph Autoencoder (MaskGAE)

Input: Graph $\mathcal{G} = (\mathcal{V}, \mathcal{E})$, encoder $f_{\theta}(\cdot)$, structure decoder $h_{\omega}(\cdot)$, degree decoder $g_{\phi}(\cdot)$, masking strategy $\mathcal{T} \in \{\mathcal{T}_{\text{edge}}, \mathcal{T}_{\text{path}}\}$, hyperparameter α ;

Output: Learned encoder $f_{\theta}(\cdot)$;

- 1: **while** not converged **do**;
 - 2: $\mathcal{G}_{\text{mask}} \leftarrow \mathcal{T}(\mathcal{G})$;
 - 3: $\mathcal{G}_{\text{vis}} \leftarrow \mathcal{G} - \mathcal{G}_{\text{mask}}$;
 - 4: $\mathbf{Z} \leftarrow f(\mathcal{G}_{\text{vis}})$;
 - 5: Calculate reconstruction loss $\mathcal{L}_{\text{GAEs}}$ over $\mathcal{G}_{\text{mask}}$ according to Eq. (1);
 - 6: Calculate regression loss \mathcal{L}_{deg} over $\mathcal{G}_{\text{mask}}$ according to Eq. (10);
 - 7: Calculate loss function $\mathcal{L} \leftarrow \mathcal{L}_{\text{GAEs}} + \alpha \mathcal{L}_{\text{deg}}$;
 - 8: Update θ, ω, ϕ by gradient descent;
 - 9: **end while**;
 - 10: **return** $f_{\theta}(\cdot)$;
-

Algorithm 2 PyTorch-style pseudocode for MaskGAE

```
# f: encoder network
# h: structure decoder network
# g: degree decoder network
# alpha: trade-off
# edge_index: visible edges of input graph
# x: node features

masked_edges, vis_edges = masking(edge_index)
num_edges = masked_edges.size(1)
z = f(x, vis_edges) # In vanilla GAE, z = f(x, edge_index)
neg_edges = negative_sampling(num_samples=num_edges)
# Calculate reconstruction loss
loss_pos = F.crossentropy(h(z, masked_edges), torch.ones(num_edges))
loss_neg = F.crossentropy(h(z, neg_edges), torch.zeros(num_edges))
loss_gaes = loss_pos + loss_neg
# Calculate regression loss as a regularizer
loss_deg = F.mse_loss(g(z), degree(masked_edges))
# Total loss for optimization
loss = loss_gaes + alpha * loss_deg
```

D More Details on Experiments

D.1 Experimental setting

Table 4: Dataset Statistics.

Dataset	# Nodes	# Edges	# Features	# Classes	Density	Split ratio (%) (Edges)	Split ratio (%) (Nodes)
Cora	2,708	10,556	1,433	7	0.144%	85/5/10	Public
CiteSeer	3,327	9,104	3,703	6	0.082%		Public
PubMed	19,717	88,648	500	3	0.023%		Public
Photo	7,650	238,162	745	8	0.407%		10/10/80
Computer	13,752	491,722	767	10	0.260%		10/10/80
arXiv	16,9343	2,315,598	128	40	0.008%		Public
MAG	736,389	10,792,672	128	349	0.002%		Public

Datasets. We conduct experiments on several well-known benchmark datasets, including three citation networks, i.e., Cora, CiteSeer, PubMed [31], two co-purchase graphs, i.e., Photo, Computer [32], as well as two large datasets arXiv and MAG from Open Graph Benchmark [14]. The datasets are collected from real-world networks belonging to different domains. For link prediction task and MGM pretraining, we randomly split the dataset with 85%/5%/10% of edges for training/validation/testing. All the models are trained on the graph with the remaining 85% existing edges. For node classification task, we adopt a 1:1:8 train/validation/test splits for Photo and Computer, and the public splits for the other 5 datasets. The detailed statistics of all datasets are summarized in Table 4.

MaskGAE setup. By default, we fix the masking ratio p to 0.7 for $\mathcal{T}_{\text{edge}}$. For $\mathcal{T}_{\text{path}}$, we randomly sample 50% of nodes from \mathcal{V} as root nodes \mathcal{R} , performing random walk [26] starting from \mathcal{R} with $n_{\text{walk}} = 2$, $l_{\text{walk}} = 4$. For all configurations, 3 GCN layers are applied for the encoder, and 2 MLP layers are applied for both structure and degree decoders. Batch normalization [15] and ELU [4] activation are applied on every hidden layer of encoder. We fix $d_h = 64$ for Cora, Citeseer, PubMed and Photo, $d_h = 128$ for Computer and MAG, $d_h = 256$ for arXiv. For α , grid search was performed over the following search space: $\{0, 1e-3, \dots, 1e-2\}$. In the self-supervised pre-training stage, we employ an Adam optimizer with an initial learning rate 0.01 and train for 500 epochs except 100 for MAG. We also use early stopping with the patience of 50, where we stop training if there is no further improvement on the validation AUC during 50 epochs.

Evaluation. We consider two fundamental tasks associated with graph representation learning: link prediction and node classification. For link prediction task, we randomly sample 10% existing edges from each dataset as well as the same number of nonexistent edges (unconnected node pairs) as testing data. For node classification task, we follow the linear evaluation scheme as introduced in [42, 53]: We first train the model in a graph with self-defined supervisions, by optimizing the objective in Eq. (11). We then *concatenate* the output of each layer as the node representation. The final evaluation is done by fitting a linear classifier (i.e., a logistic regression model) on top of the frozen learned embeddings without flowing any gradients back to the encoder. Note that we did not compare with the two related works MGAE [35] and GMAE [2] in node classification task as the authors’ codes are not released and they adopt a rather different experimental setting.

Software and hardware infrastructures. Our framework is built upon PyTorch [24] and PyTorch Geometric [6], which are open-source software released under BSD-style ⁵ and MIT ⁶ license, respectively. All datasets used throughout experiments are publicly available in PyTorch Geometric library. All experiments are done on a single NVIDIA A100 GPU (with 40GB memory).

⁵<https://github.com/pytorch/pytorch/blob/master/LICENSE>

⁶https://github.com/pyg-team/pytorch_geometric/blob/master/LICENSE

D.2 Ablation study

We perform ablation studies over the key components of MaskGAE to understand their functionalities more thoroughly. We report the performance of MaskGAE on node classification performance by varying one and fixing others as optimal values.

Ablation on $\mathcal{T}_{\text{edge}}$. We first study how the masking ratio improves or degrades the performance. We adopt a large masking ratio (i.e., $p \geq 0.5$) for the sake of training efficiency, following [12]. From Figure 4, we can see that MaskGAE_{edge} consistently outperforms vanilla GAE, which aligns with our theoretical justifications that MGM improves the self-supervised learning scheme. By increasing the masking ratio from 0.5 to 0.7, the accuracy is smoothly improved by $\sim 0.2\%$ on all benchmarks. When p reaches a critical value, e.g., 0.7, the best performance is achieved.

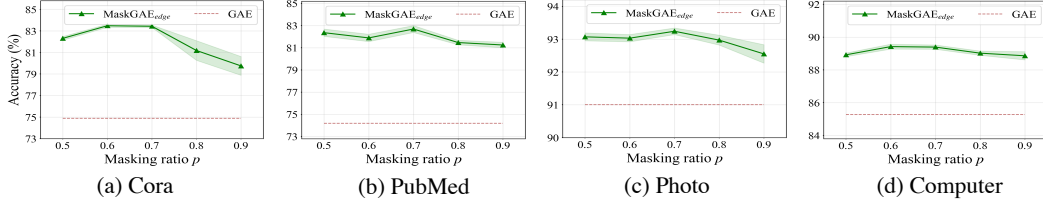


Figure 4: Effect of masking ratio p .

Ablation on $\mathcal{T}_{\text{path}}$. The number of masked edges by $\mathcal{T}_{\text{path}}$ is jointly controlled by n_{walk} and l_{walk} , as we fix \mathcal{R} as 50% of nodes sampled from \mathcal{V} . Figure 5 shows the node classification performance of MaskGAE_{path} on node classification task using different n_{walk} and l_{walk} . The plots suggest that both parameters contribute equally to the downstream performance. As shown, two parameters that are too large or too small can lead to poor performance. In this regard, reasonable values of n_{walk} and l_{walk} (e.g., $n_{\text{walk}} = 2$ and $l_{\text{walk}} = 4$) are required to learn useful representations.

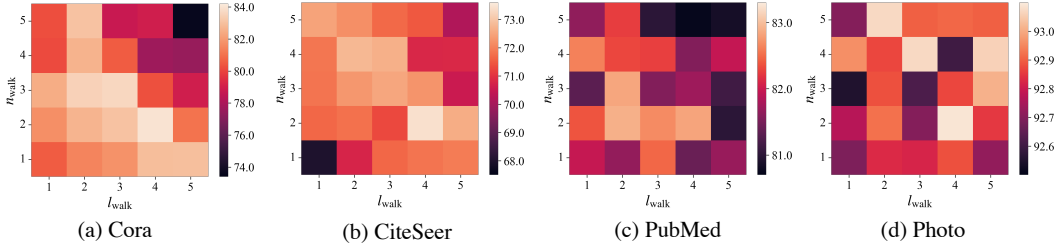


Figure 5: Effect of n_{walk} and l_{walk} .

Effect of α . We further investigate whether \mathcal{L}_{deg} improves the performance as an auxiliary loss by varying the trade-off hyper-parameter α . Figure 6 shows the classification accuracy of both MaskGAE variants w.r.t. different α on four benchmarks. We can see that the performance is boosted when $\alpha > 0$ particularly for MaskGAE_{path}. This indicates that \mathcal{L}_{deg} is important as it contributes to learning good representations for downstream tasks. However, a large α results in a poor performance as the model might overfit the structure information.

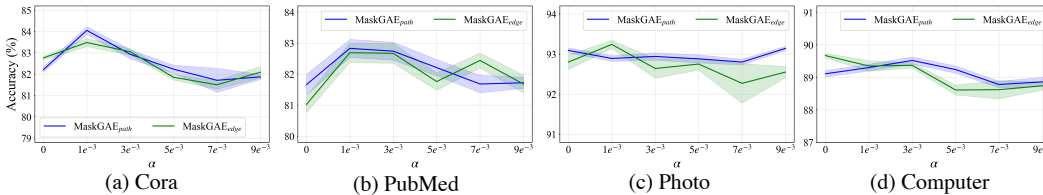


Figure 6: Effect of α .

Effect of embedding size. Figure 7 ablates the effect of varying embedding size. Embedding size is important for graph representation learning, which reflects the effectiveness of information compression. Compared to contrastive methods [42, 22, 55], MaskGAE does not benefit significantly from a large embedding dimension. In contrast, we notice a performance drop for MaskGAE_{path} as the embedding size increases in most cases. An interesting finding is that MaskGAE_{path} obtains its best performance with a 64-dimensional embedding in most benchmarks, while other methods generally need much larger dimensions to achieve their best performance, as reported in [22]. An interesting finding is that a small embedding size (64 on most benchmarks) is sufficient for MaskGAE_{path}. It also shows that a large range of embedding sizes (e.g., 128-512) perform equally well for MaskGAE_{edge}. This indicates that the representations learned by MaskGAE are informative and discriminant for downstream tasks as a small embedding size is required.

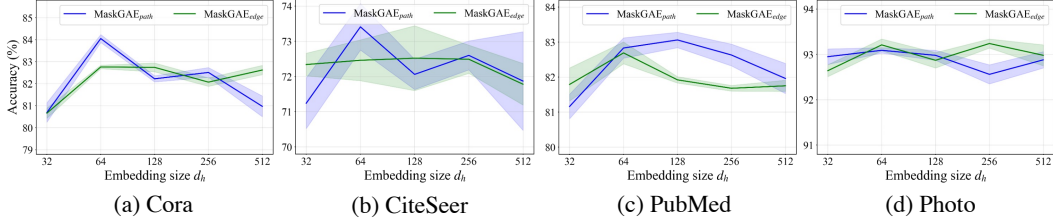


Figure 7: Effect of embedding size d_h .

E Discussions

On the negative edge sampling procedure. To strictly adhere to the infomax paradigm, we need the negative samples pairs to be independently drawn from the marginals. The original GAE objective (1) is therefore a biased estimate of the population objective (3) since the negative samples are drawn from unconnected node pairs. However, the estimation bias does not affect the analysis: denote the true negative sampling distributions as P_{UV}^- , then following the procedure in [40], we can show that following optimizer

$$\tilde{h}_* \in \arg \min_{h \in \mathcal{H}} - \left(\mathbb{E}_{u,v \sim P_{UV}} \log h(u,v) + \mathbb{E}_{u',v' \sim P_{UV}^-} \log(1 - h(u',v')) \right) \quad (28)$$

satisfies that

$$D_{\text{KL}}(P_{UV} || P_{UV}^-) = \mathbb{E}_{u,v \sim P_{UV}} \tilde{h}_*(u,v) - \log \mathbb{E}_{u,v \sim P_{UV}^-} (e^{\tilde{h}_*(u,v)}). \quad (29)$$

Since the Kullback-Leibler divergence enjoys the chain rule [27], the discussion in § 4 follows the modeling paradigm under the true negative sampling process as well, with some modification over the definition of MI.

Limitations of the work. Despite the theoretical grounds and the promising experimental justifications, our work might potentially suffer from some limitations: (i) As like existing augmentation-based contrastive methods, performing masking (a kind of augmentation) on the graph structure would hurt the semantic meaning of some graphs, such as biochemical molecules [29, 54]. (ii) MaskGAE is mainly based on the homophily assumption, a basic assumption in the literature of graph-based representation learning. However, such an assumption may not always hold in heterophilic graphs, where the labels of linked nodes are likely to differ.

Potential negative societal impact. Self-supervised learning on graphs is an important technique to make use of rich unlabeled data and can be applied to many fields such as financial networks [46] and molecular biology [29, 54]. Our work presents a self-supervised framework for learning effective and generalizable node representations. These representations enable learning robust classifiers with limited data and thus facilitate applications in many domains where annotations are expensive or difficult to collect. Just like any machine learning algorithm can be used for good it can also be used for harm. For example, an immediate application of this work is to conveniently construct a pretrained dataset by random crawling data from elsewhere. This is economic and beneficial for research purposes, but would potentially risk privacy and license issues in many security-sensitive

situations. This would be the potential concerns and negative societal impact of our work. The line of self-supervised learning works, including this paper, are not immune to such misuse. Currently, we have no solution for such a general problem but we are aware that this needs to be addressed in future work.